Int. J. Electrochem. Sci., 14 **(2019)** 7380 – 7388, doi: 10.20964/2019.08.31

International Journal of
ELECTROCHEMICAL
SCIENCE
www.electrochemsci.org

Novel Detection of Acrylamide by Electrochemiluminescence Sensor and Optical Imaging Analysis

Xin Yang [1,+], *Peng Pan* [1,+], *Li Tu* [1,+], *Zhenyu Liao* [2,3], *Huimin Niu* [1], *Chuanlai Zang* [1], *Mingchen Li* [1], *Jun Liu* [1,*], *Zhengchun Yang* [1,*], *Yangyang Qi* [1,*], *Jun Wei* [1,4], *Kwok Wei Shah* [5]

[1] School of Electrical and Electronic Engineering, Advanced Materials and Printed Electronics Center, Tianjin Key Laboratory of Film Electronic & Communication Devices, Tianjin University of Technology, Tianjin 300384, China
[2] Pony Testing International Group, Tianjin 300110, China
[3] Tianjin Food Safety Inspection Technology Institute, Tianjin 300308, China
[4] Singapore Institute of Manufacturing Technology, Agency for Science, Technology and Research (A*STAR),71 Nanyang Drive, 638075, Singapore
[5] School of Design and Environment, Department of Building, National University of Singapore, 4 Architecture Drive, 117566, Singapore
[+]These authors contributed equally to this work.
[*]E-mail: cloudlj@163.com, yangzhengchuntjut@163.com, qyyqyqwx@163.com

Received: 10 April 2019 / *Accepted:* 20 June 2019 / *Published:* 30 June 2019

Acrylamide, a carcinogen with debilitating effects on human health, was detected by electrochemiluminescence (ECL) measurement using $Ru(bpy)_3^{2+}$ as the luminophore. Under the optimum conditions, Pt electrode as the working electrode showed a superior linear detection in the range 5 μM–10 mM, with a detection limit of 1.2 μM (S/N = 3). Moreover, a remote wireless camera was employed to collect the digital images of the ECL emission. These images were converted from RGB (Red, Green, Blue) model to HSV (Hue, Saturation, Value) model using the MATLAB software. It was found that Value (V) in the HSV model had a linear relationship with the logarithm of the acrylamide concentration, suggesting that acrylamide could be detected in levels of 5 μM using optical imaging. The ECL method for detecting acrylamide was proved to be simple and convenient. This is expected to lead to the development of a novel acrylamide detection method for food safety and other fields.

Keywords: electrochemiluminescence; acrylamide detection; optical imaging

1. INTRODUCTION

Acrylamide is a highly water soluble, white or pale-yellow crystal. A large amount of acrylamide is produced after cooking starchy foods at high temperatures[1, 2]. A number of studies

have been conducted on the mechanism of formation of acrylamide[3-5]. However, acrylamide is a potential carcinogen that effects the human nervous system and reproductive system[6]. Hence, it is crucial to monitor the presence of acrylamide, considering the aspect of food safety.

The existing methods for detecting acrylamide are as follows. Gas chromatography has been widely used in detecting acrylamide[7, 8]. Although this technique has good detection sensitivity and accuracy, bromine used for the chromatographic analysis is volatile, corrosive, and toxic, and hence, is against the concept of green chemistry. Moreover, the expensive technology and equipment limit its applications. The use of high performance liquid chromatography has simplified this analysis[9, 10]. This method is carried out at room temperature and overcomes the thermal instability of acrylamide. However, the instrumentation is expensive, and the detection time is long. Furthermore, pre-column derivatization-gas chromatography–mass spectrometry developed to detect acrylamide in food is more sensitive and accurate than gas chromatography[11, 12]. However, even this technique requires complex instrumentation and complicates its operations. Enzyme-linked immunosorbent assays have been shown to be highly specific for acrylamide[13]. The method is cost-effective and has a relatively short detection time. However, the sensitivity needs to be improved. Moreover, this method involves the preparation of antibodies, which may be difficult at times. In summary, these detection methods require relatively complicate pre-processing process and long analysis time, which are not suitable for on-site and rapid detection.

Measurement of electrochemiluminescence (ECL) is an outstanding method for sensing applications[14, 15], which has been widely used in drug analysis[16], amino acid analysis[17], DNA probe analysis[18] and the field of enzyme biosensors[19]. $Ru(bpy)_3^{2+}$ is a common luminophore in ECL measurements[20, 21]. Amines can be employed as reducing agent for $Ru(bpy)_3^{2+}$, such as tripropylamine[22, 23] and melamine[24]. Therefore, acrylamide, also a kind of amine, can be used as a reducing agent for reacting with $Ru(bpy)_3^{2+}$.

In this work, acrylamide was successfully detected in phosphate buffer saline (PBS) by ECL measurement using $Ru(bpy)_3^{2+}$ as the luminophore. The method was linear over a wide range, involved relatively inexpensive instrument, and was cost-effective and operationally simple. Pt electrode was used as the working electrode, and it showed a superior linear detection in the range 5 μM–10 mM, with a detection limit of 1.2 μM (S/N=3). In addition, the digital images of ECL emission were collected by remote wireless camera, which were converted from RGB (Red, Green, Blue) model to HSV (Hue, Saturation, Value) model using the MATLAB software. When these images were captured as 200×200 pixels, there was a good linear relationship between Value (V) and the logarithm of the acrylamide concentration. Thus, the combination of these two methods (optical imaging and ECL) is a promising method for ECL sensing and is expected to provide a new way for detecting acrylamide in food safety and other related fields.

2. EXPERIMENTAL DETAIL

2.1 Chemicals and reagents

$Ru(bpy)_3^{2+}$ and acrylamide were obtained from Titan Scientific Co., Ltd. (Shanghai, China). 10 mM PBS was procured from RUICHU Biotech Co., Ltd. (Shanghai, China). Deionized water obtained from an EASY Ultra-pure Water system was used in all the experiments, unless otherwise stated.

2.2 ECL measurements and optical image generation

All ECL measurements were performed at room temperature (~25 °C) by the MPI-EII (Remex Electronic Instrument Co., Ltd. Xi'an, China) detection system. A three-electrode system consisting of an Ag/AgCl electrode (saturated KCl solution) as the reference electrode, Pt electrode as the working electrode, and a counter electrode was employed. The ECL was monitored by cyclic voltammetry (CV) in the voltage range −1.1–1.3 V and at a scan rate of 0.1 $V \cdot s^{-1}$. The photomultiplier tube was set at 800 V. The ECL signals were collected by a H.264-1080P remote wireless hidden camera. The obtained images were analyzed using MATLAB.

3. RESULTS AND DISCUSSION

3.1 Optimization of ECL measurement conditions

To acquire the optimum conditions for detecting acrylamide, a few experimental factors, such as pH of PBS and scan rate in CV method were examined at room temperature. Previous studies suggest that the ECL intensity of acrylamide was affected by amino protonation[25, 26], and this was related to the pH of the solution. Therefore, it was necessary to study the ECL in PBS of varying pH. Fig. 1a and Fig. 1b describe the influence on the ECL intensity in the pH range 3–11. Fig. 1c shows that the ECL intensity increases from pH 3 to pH 7 and decreases with further increase in the pH. The ECL intensity reaches its maximum at pH 7. Therefore, PBS with pH=7 was employed for further studies.

The change in ECL at different scan rates is shown in Fig. 1d and Fig. 1e. Fig. 1f predicts that the ECL intensity is maximum in the range 0.02–0.1 $V \cdot s^{-1}$ and then decreases from 0.1 to 0.2 $V \cdot s^{-1}$. Based on the previous report[27], when the scan rate is in the range of 0.02-0.1 $V \cdot s^{-1}$, the excited-state substance is insufficiently produced at low scan rate. As the reaction progresses, the co-reactant is accumulated near the electrodes. When the scan rate increases, for instance, up to 0.1 $V \cdot s^{-1}$, the rate of migration of electrons increases. The concentration of the excited state luminophore is increased, and hence, the ECL intensity is enhanced. When the scan rate exceeds 0.1 $V \cdot s^{-1}$, the amount of co-reactant near electrode surface cannot cope with the fast ECL reaction the fast ECL reaction, and the ECL intensity decreases. Therefore, a scan rate of 0.1 $V \cdot s^{-1}$ was employed for further experiments.

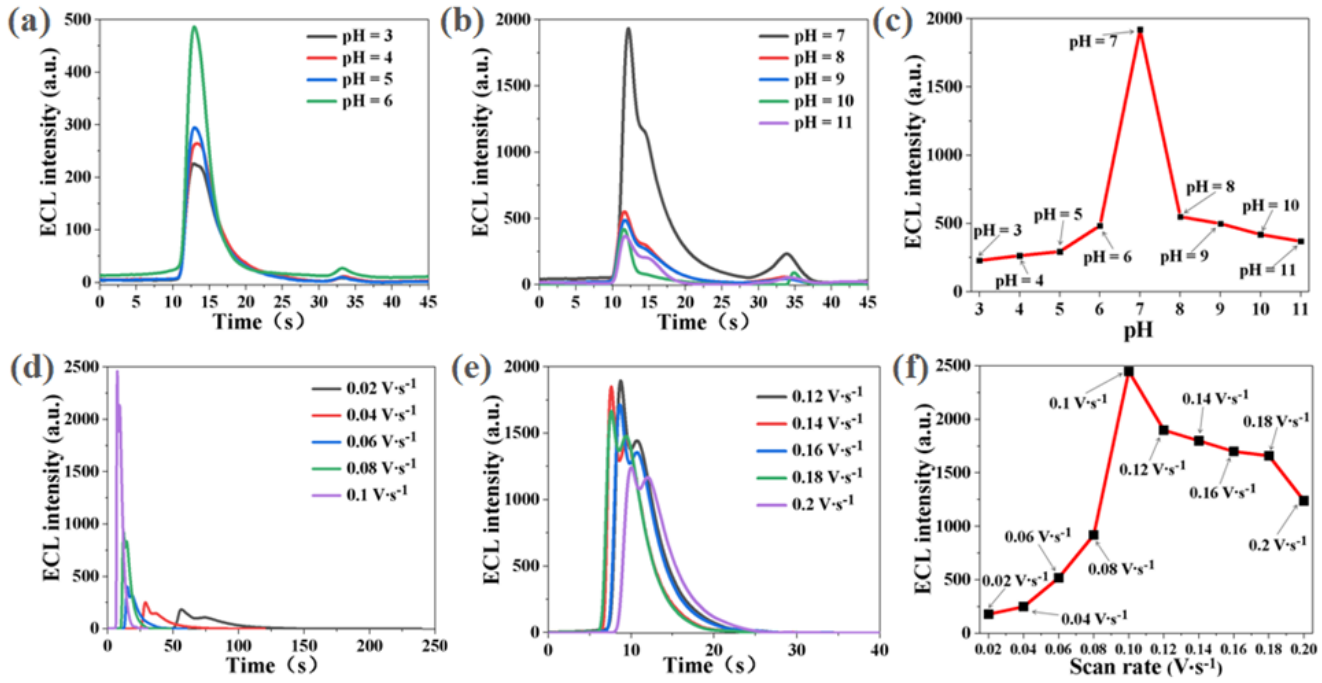

Figure 1. (a) and (b) Effect of pH in different pH ranges. (c) Variation in ECL intensity over the entire pH range. (d) and (e) Effect of scan rate on the ECL intensity. (f) Variation in ECL intensity over the entire scan range.

Fig. 2 illustrates the ECL emission profiles and CV curves in the presence and absence of acrylamide. Both the peaks emerge at about 1.1 V. The ECL intensity in the presence of acrylamide is significantly enhanced compared with that in its absence.

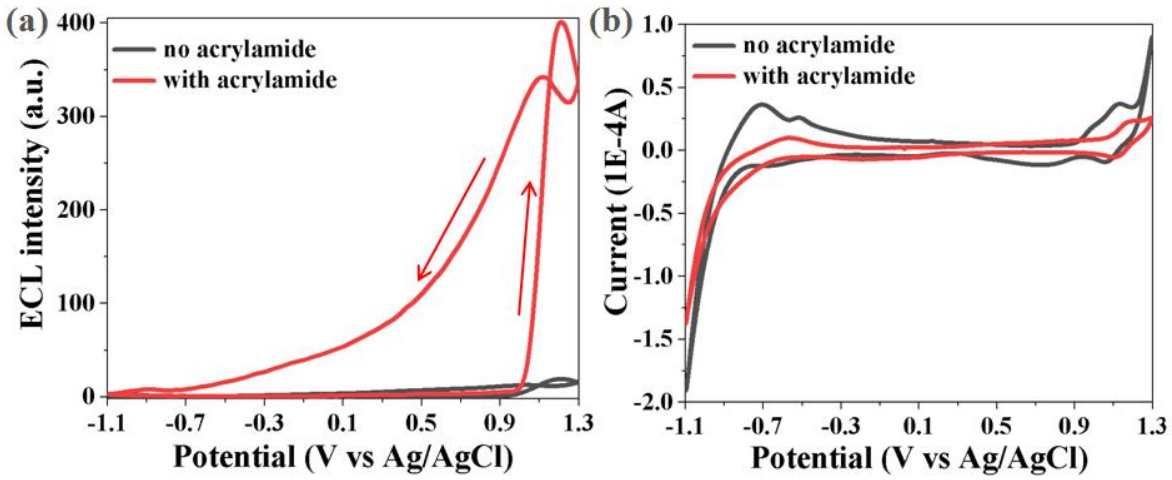

Figure 2. (a) ECL intensity vs potential in the presence and absence of acrylamide. (b) CV curves in the presence and absence of acrylamide (scan rate: 0.1 $V \cdot s^{-1}$, buffer: PBS, pH: 7, photomultiplier tube: 800 V)

It is well known that $Ru(bpy)_3^{2+}$ can react with amines such as tripropylamine[28], melamine[29], and dopamine[30] to emit ECL. Therefore, the mechanism of ECL emission in the presence of acrylamide can be inferred based on this. Fig. 3a shows the mechanism of ECL emission

of $Ru(bpy)_3^{2+}$ with acrylamide. According to a previous report[31, 32], when the scanning potential is close to 1.1 V, acrylamide is oxidized. $Ru(bpy)_3^{2+}$ is also oxidized to $Ru(bpy)_3^{3+}$, which reacts with oxidized acrylamide to obtain the excited state $Ru(bpy)_3^{2+*}$. When the unstable excited state $Ru(bpy)_3^{2+*}$ returns to the ground state $Ru(bpy)_3^{2+}$, a significant ECL signal can be observed. The reaction mechanism for $Ru(bpy)_3^{2+}$ with acrylamide is represented by eqs 1−4, where D represents acrylamide:

$$Ru(bpy)_3^{2+} - e^- \rightarrow Ru(bpy)_3^{3+} \quad (1)$$

$$D - e^- \rightarrow D^{\cdot} + H^+ \quad (2)$$

$$Ru(bpy)_3^{3+} + D^{\cdot} \rightarrow Ru(bpy)_3^{2+*} + \text{other products} \quad (3)$$

$$Ru(bpy)_3^{2+*} \rightarrow Ru(bpy)_3^{2+} + h\nu \quad (4)$$

In addition, the stability and reproducibility under the optimized conditions (Fig. 3b) were found to be satisfactory.

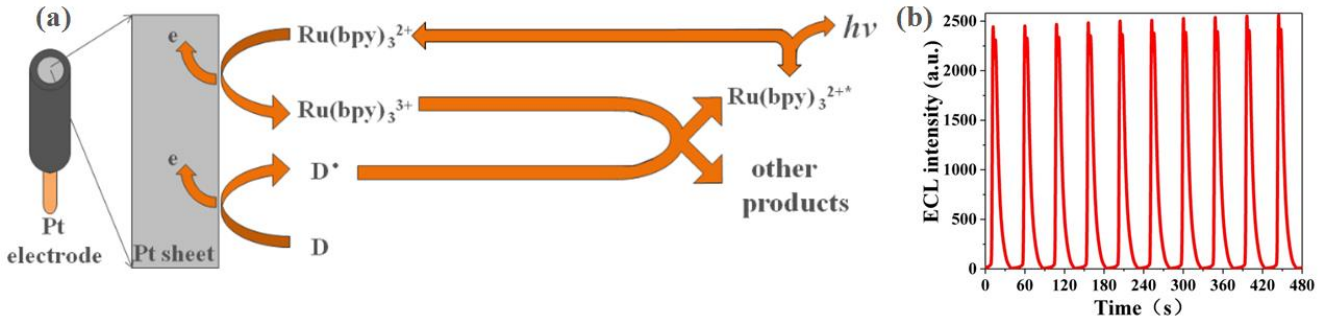

Figure 3. (a) The reaction scheme for ECL of $Ru(bpy)_3^{2+}$ with acrylamide (D represents acrylamide); (b) ECL stability under 10 continuous CV scans (scan rate: 0.1 $V \cdot s^{-1}$, buffer: PBS, pH: 7, photomultiplier tube: 800 V)

This mechanism is similar to that for other well-known co-reactants such as tripropylamine. The presence of a return wave for the reduction of $Ru(bpy)_3^{3+}$ to $Ru(bpy)_3^{2+}$, after the appearance of the first peak, indicates that the reaction between $Ru(bpy)_3^{3+}$ and acrylamide is less efficient. This results in the lower ECL intensity[33]. The above experiment confirms that acrylamide can be used as a reducing agent for the redox reaction with $Ru(bpy)_3^{2+}$ and can be detected by ECL measurement.

3.2 Determination of acrylamide

Under the optimized conditions, ECL was monitored by CV in voltage range −1.1–1.3 V and scan rate of 0.1 $V \cdot s^{-1}$. Fig. 4a illustrates the relationship of ECL intensity and acrylamide concentration. The ECL intensity is continuously enhanced with increasing acrylamide concentration. Fig. 4b shows that fitted curve for the same between 5 μM and 10 mM. It can be seen that ECL intensity has a good linear relationship with the logarithm of the acrylamide concentration. The detection limit in this range was 1.2 μM. The resulting equation is $Y_2 = 700.15299X_2 - 310.20364$, with $R^2 = 0.99155$. A comparison between this work and some previous studies for detecting acrylamide is listed in Table 1. Although the detection limits of these methods are similar, the method provided in this study is more convenient. The interference immunity of acrylamide is shown in Fig. 5. The same

concentrations (1 mM) of urea, uric acid and glucose were used for ECL under the above conditions. It was found that the CV curves of acrylamide and other substances were different, indicating that acrylamide could be distinguished from these compounds.

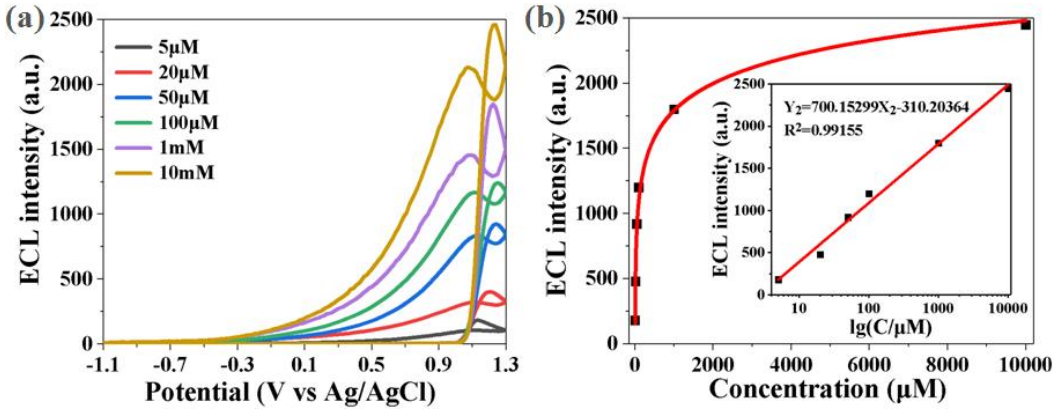

Figure 4. (a) ECL curves with different concentrations of acrylamide and (b) ECL intensity vs logarithm of acrylamide concentration (scan rate: 0.1 $V \cdot s^{-1}$, buffer: PBS, pH: 7, photomultiplier tube: 800 V)

Table 1. Comparison between this work and some previous studies for detecting acrylamide

Methods	Detection System	Limit of detection	References
micellar electrokinetic chromatography (MEKC)	Capillary electrophoresis	100μg·L^{-1}	[34]
biomimetic enzyme-linked immunosorbent assay (BELISA)	Hydrophilic imprinted membrane	85μg·L^{-1}	[35]
ECL (based on Pt)	MPI-EII	1.2μM	This work

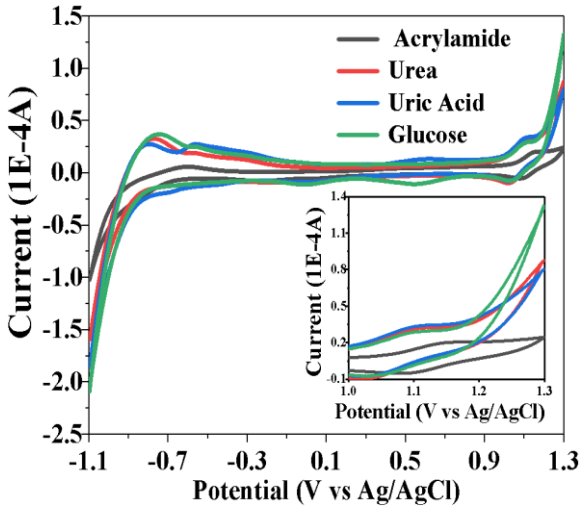

Figure 5. several different CV curves, including 1 mM acrylamide, 1 mM urea, 1 mM uric acid, 1 mM glucose (scan rate: 0.1 $V \cdot s^{-1}$, buffer: PBS, pH: 7, photomultiplier tube: 800 V)

$Ru(bpy)_3^{2+}$ emits an orange-red visible light (λ = 620 nm) in ECL[36]. Therefore, The optical images at different acrylamide concentrations were converted from RGB (Red, Green, Blue) model to HSV (Hue, Saturation, Value) model using MATLAB software[37-39]. Value (V) in the HSV model was investigated, and the results are shown in Fig. 6. The X and Y axes are used to indicate the size of the picture. The Z axis is used to describe Value (V). The yellow portion represents the bright part of the image. It is found that the value of the image enhances significantly as the acrylamide concentration increases. Afterwards, a related algorithm is used to automatically cut out the fixed area of 200 × 200 pixels in the yellow portion of each image. The output images are shown in the Fig. 7a. Fig. 7b shows the relationship between Value (V) and the logarithm of the acrylamide concentration. The resulting equation is $Y_2=0.10458X_2+0.01653$, with R^2 = 0.98013, indicating an excellent linear relationship between the two parameters. In the future, smartphones can be applied to realize real-time processing, which would make the micro-detection of substances simpler and faster.

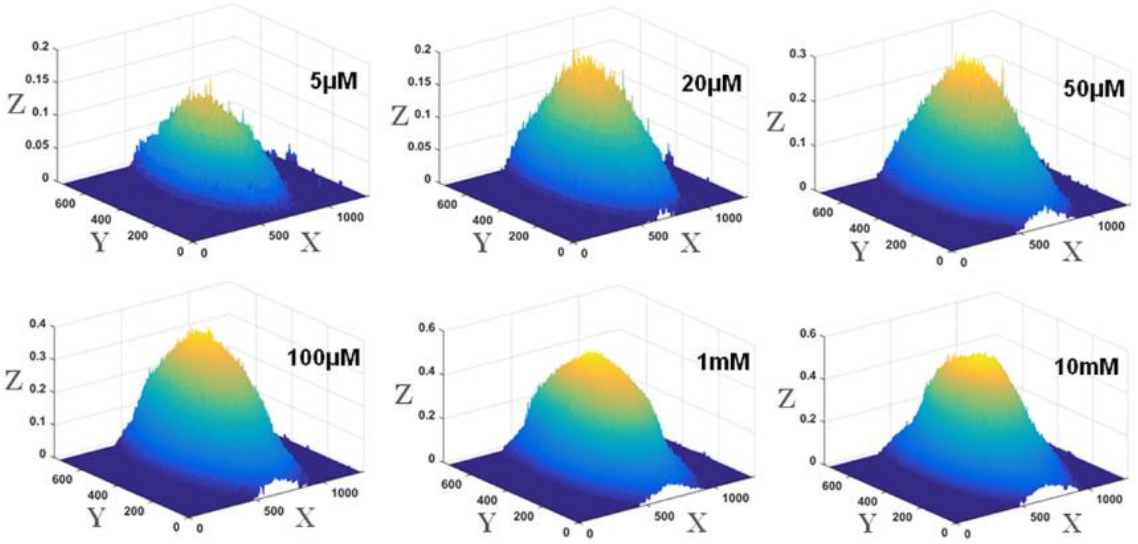

Figure 6. Value (V) at different acrylamide concentrations obtained using the MATLAB software

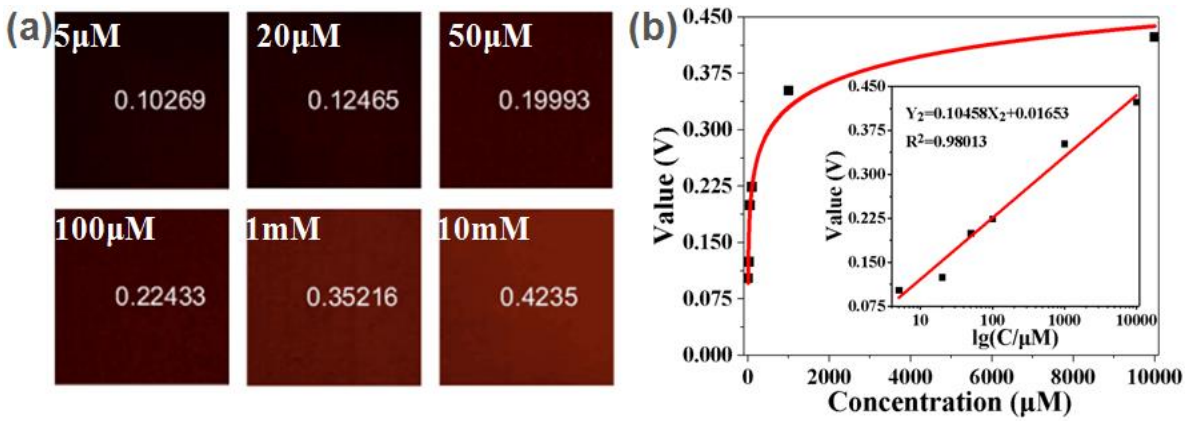

Figure 7. (a) 200×200 pixels images of ECL from camera obtained for various concentrations of acrylamide (the value of 5μM is 0.10269, the value of 20μM is 0.12465, the value of 50μM is 0.19993, the value of 100μM is 0.22433, the value of 1mM is 0.35216, the value of 10mM is 0.4235); (b) Value (V) vs logarithm of acrylamide concentration

4. CONCLUSIONS

In summary, the detection of acrylamide by ECL measurement and optical imaging were studied. The ECL intensity under different acrylamide concentrations were obtained by CV. The optical images were analyzed with a series of acrylamide concentrations using the MATLAB software. The ECL intensity and Value (V) of the images have a good linear relationship with the logarithm of the acrylamide concentration. The linear detection range is from 5μM to 10mM with a detection limit of 1.2μM (S/N=3). The stability and reproducibility were satisfactory. Therefore, the combination of ECL measurement and optical imaging for detecting acrylamide was simple and convenient. It is expected to lead to the development of a novel acrylamide detection method for food safety and other fields.

ACKNOWLEDGEMENTS
This research was funded by Student's Platform for Innovation and Entrepreneurship Training Program (Grant No. 201810060186, 201710060046), Tianjin Development Program for Innovation and Entrepreneurship, Tianjin Natural Science Foundation (Grant No. 18JCZDJC99800), National Natural Science Foundation of China (51502203), Tianjin Young Overseas High-level Talent Plans (Grant No. 01001502) and Tianjin Science and Technology Foundation (Grant No. 17ZXZNGX00090).

References

1. M. Palermo, V. Gokmen, B. De Meulenaer, Z. Ciesarova, Y. Zhang, F. Pedreschi, V. Fogliano, *Food Funct.*, 7 (2016) 2516-2525.
2. V.A. Yaylayan, R.H. Stadler, *J. AOAC Int.*, 88 (2005) 262-267.
3. D.R. Lineback, J.R. Coughlin, R.H. Stadler, Acrylamide in Foods: A Review of the Science and Future Considerations, in: M.P. Doyle, T.R. Klaenhammer (Eds.) Annual Review Of Food Science And Technology, Vol 3, vol. 3, Annual Reviews, Palo Alto, 2012, pp. 15-35.
4. E.M. Lodolini, M. Cabrera-Banegil, A. Fernandez, J. Delgado-Adamez, R. Ramirez, D. Martin-Vertedor, *Food Chem.*, 286 (2019) 250-259.
5. R.H. Stadler, I. Blank, N. Varga, F. Robert, J. Hau, P.A. Guy, M.-C. Robert, S. Riediker, *Nature*, 419 (2002) 449-450.
6. V. Matoso, P. Bargi-Souza, F. Ivanski, M.A. Romano, R.M. Romano, *Food Chem.*, 283 (2019) 422-430.
7. C. Carrero-Carralero, J. Escobar-Arnanz, M. Ros, S. Jimenez-Falcao, M.L. Sanz, L. Ramos, *Talanta*, 195 (2019) 800-806.
8. Z. Hadian, S. Eslamizad, H. Yazdanpanah, *Iran. J. Pharm. Res.*, 18 (2019) 275-285.
9. M.B. Galuch, T.F.S. Magon, R. Silveira, A.E. Nicacio, J.S. Pizzo, E.G. Bonafe, L. Maldaner, O.O. Santos, J.V. Visentainer, *Food Chem.*, 282 (2019) 120-126.
10. M. Zhu, L. Yang, W. Zhang, C. Cai, X. Zhou, *Se pu = Chinese journal of chromatography*, 37 (2019) 189-193.
11. Z.M. Geng, R. Jiang, M. Chen, *J. Food Compos. Anal.*, 21 (2008) 178-182.
12. M.V. Russo, P. Avino, A. Centola, I. Notardonato, G. Cinelli, *Food Chem.*, 146 (2014) 204-211.
13. Y. Ma, X.L. Shen, Q. Zeng, H.S. Wang, L.S. Wang, *Talanta*, 164 (2017) 121-127.
14. A. Sadowska-Rociek, M. Surma, E. Cieslik, *Roczniki Panstwowego Zakladu Higieny*, 69 (2018) 127-137.

15. M. Wei, C.L. Wang, E.S. Xu, J. Chen, X.L. Xu, W. Wei, S.Q. Liu, *Food Chem.*, 282 (2019) 141-146.
16. D.D. Fang, M.A. Pan, H. Yi, H. Dai, Z.S. Hong, X.Q. Zheng, Y.Y. Lin, *Sens. Actuator B-Chem.*, 286 (2019) 608-615.
17. Z.Y. Shang, C.F. Han, Q.J. Song, *Chin. J. Anal. Chem.*, 42 (2014) 904-908.
18. Y.F. Wang, W.W. Guo, N.Q. Jia, *ChemElectroChem*, 5 (2018) 3786-3792.
19. G.T. Jie, Q. Zhou, G.F. Jie, *Talanta*, 194 (2019) 658-663.
20. D.W. Fan, X. Liu, C.Z. Bao, J.H. Feng, H. Wang, H.M. Ma, D. Wu, Q. Wei, *Biosens. Bioelectron.*, 129 (2019) 124-131.
21. R. Heidari, J. Rashidiani, M. Abkar, R.A. Taheri, M.M. Moghaddam, S.A. Mirhosseini, R. Seidmoradi, M.R. Nourani, M. Mahboobi, A.H. Keihan, H. Kooshki, *Biosens. Bioelectron.*, 126 (2019) 7-14.
22. Y.Q. Feng, F. Sun, N.N. Wang, J.P. Lei, H.X. Ju, *Analytical Chemistry*, 89 (2017) 7659-7666.
23. X. Shan, Y. Pan, X. Chen, W. Wang, Z. Chen, *Analytical sciences : the international journal of the Japan Society for Analytical Chemistry*, (2019).
24. E. Daviddi, A. Oleinick, I. Svir, G. Valenti, F. Paolucci, C. Amatore, *ChemElectroChem*, 4 (2017) 1719-1730.
25. C. Cheng, Y. Huang, X. Tian, B. Zheng, Y. Li, H. Yuan, D. Xiao, S. Xie, M.M.F. Choi, *Analytical Chemistry*, 84 (2012) 4754-4759.
26. D.F. Feng, Y.Y. Wu, X.C. Tan, Q.Y. Chen, J. Yan, M. Liu, C.H. Ai, Y.N. Luo, F.K. Du, S.G. Liu, H.Y. Han, *Sens. Actuator B-Chem.*, 265 (2018) 378-386.
27. H. Dai, Y.W. Chi, X.P. Wu, Y.M. Wang, M.D. Wei, G.N. Chen, *Biosens. Bioelectron.*, 25 (2010) 1414-1419.
28. Q.Q. Gai, D.M. Wang, R.F. Huang, X.X. Liang, H.L. Wu, X.Y. Tao, *Biosens. Bioelectron.*, 118 (2018) 80-87.
29. N. Lu, W.C. Wang, X.H. Chen, Z.D. Chen, *Int. J. Electrochem. Sci.*, 12 (2017) 4035-4043.
30. H.M. Wang, C.C. Wang, A.J. Wang, L. Zhang, X.L. Luo, P.X. Yuan, J.J. Feng, *Sens. Actuator B-Chem.*, 281 (2019) 588-594.
31. R.V. Bensasson, C. Salet, *C.R. Hebd. Seances Acad. Sci. B, Sci. Phys.*, 289 (1979) 41-43.
32. J. Ferguson, E.R. Krausz, *Chem. Phys. Lett.*, 93 (1982) 21-25.
33. F. Jameison, R.I. Sanchez, L. Dong, J.K. Leland, D. Yost, M.T. Martin, *Analytical Chemistry*, 68 (1996) 1298-1302.
34. T. Wenzl, L. Karasek, J. Rosen, K.E. Hellenaes, C. Crews, L. Castle, E. Anklam, *J. Chromatogr. A*, 1132 (2006) 211-218.
35. Q. Sun, L.H. Xu, Y. Ma, X.G. Qiao, Z.X. Xu, *J. Sci. Food Agric.*, 94 (2014) 102-108.
36. L.L. Xue, L.H. Guo, B. Qiu, Z.Y. Lin, G.N. Chen, *Electrochem. Commun.*, 11 (2009) 1579-1582.
37. J.T. Cao, Y.L. Wang, J.J. Zhang, Y.X. Dong, F.R. Liu, S.W. Ren, Y.M. Liu, *Analytical Chemistry*, 90 (2018) 10334-10339.
38. F.K. Du, H. Zhang, X.C. Tan, J. Yan, M. Liu, X. Chen, Y.Y. Wu, D.F. Feng, Q.Y. Chen, J.M. Cen, S.G. Liu, Y.Q. Qiu, H.Y. Han, *Biosens. Bioelectron.*, 106 (2018) 50-56.
39. A.K. Korayem, S. Ghamami, Z. Bahrami, *Signal Image Video Process.*, 13 (2019) 281-287.